INTERNATIONAL JOURNAL OF ADAPTIVE CONTROL AND SIGNAL PROCESSING
Int. J. Adapt. Control Signal Process. 2016; **30**:1478–1493
Published online 5 October 2015 in Wiley Online Library (wileyonlinelibrary.com). DOI: 10.1002/acs.2630

Adaptive robust attitude control for UAVs – Design and experimental validation

Abdelhamid Chriette[1], Franck Plestan[1,*,†], Herman Castañeda[2], Madhumita Pal[1], Mario Guillo[3], Marcin Odelga[3], Sujit Rajappa[3] and Rohit Chandra[3]

[1]*LUNAM Université, Ecole Centrale de Nantes, IRCCyN UMR CNRS 6597, Nantes, France*
[2]*Faculty of Mechanical and Electrical Engineering (FIME) of The Autonomous University of Nuevo Leon (UANL), Monterrey, Mexico*
[3]*Ecole Centrale de Nantes, Nantes, France*

SUMMARY

The main contribution of the paper is to propose a scheme of attitude controller for a class of unmanned aerial vehicles based on an adaptive version of the super-twisting algorithm. This controller is based on a very recent second-order sliding mode controller, which is robust in spite of uncertainties and perturbations, ensures finite time convergence, reduces the chattering, increases the accuracy, and does not require time derivative of the sliding variable. A very important feature of the controller is its adaptive gain, which allows to design the controller without knowing bounds of the uncertainties and perturbations. This controller is validated by experimental results. Comparisons versus PID-based controller are made in order to evaluate the robustness of the closed-loop system when similar perturbations are acting. Copyright © 2015 John Wiley & Sons, Ltd.

Received 13 February 2015; Revised 21 July 2015; Accepted 26 August 2015

KEY WORDS: second-order sliding mode; adaptive control; attitude control

1. INTRODUCTION

Many works have been published during the last decade on robust controllers' design for aerial unmanned autonomous vehicles. In this paper, the attention is focused on the attitude control of such systems. Given this focus, the experimentations are made on an experimental set-up, which is well adapted on the evaluation of attitude control of flying systems. The advantages of this experimental system, the 3DOF Quanser helicopter [1], are its reasonable small size, which allows to test some control laws with a high level of safety, and the possibility to evaluate advanced attitude controllers versus perturbations (thanks to the use of domestic fans). Without being exhaustive, the following list of previously published results [2–7] shows that many works have been made for the design of linear/nonlinear attitude controllers. Note that all these works have made some hypothesis on the structural properties of the system (for example, controllers based on singular perturbation theory [8–10]); on the mechanical architecture, however, all these assumptions highly reduce the realism of the simulations. In the first part of the current paper, a complete attitude mode is proposed in order to acquire an efficient simulator. However, it is necessary to be fully aware that, even if the used assumptions are quite reduced, the model presents uncertainties and perturbations. The design of robust controllers is then required. In this paper, a nonlinear adaptive robust attitude controller is developed for the 3DOF helicopter prototype. The scheme of the controller

*Correspondence to: Franck Plestan, LUNAM Université, Ecole Centrale de Nantes, IRCCyN UMR CNRS 6597, Nantes, France.
†E-mail: franck.plestan@irccyn.ec-nantes.fr

has been initially developed in [11] and used in [12, 13]: it allows to decouple the system thanks to the introduction of both virtual inputs for travel and elevation angles and to design a desired reference for the pitch angle. This approach is adapted to user's expectations. Indeed, in standard working conditions, the user can provide elevation and travel desired trajectories with respect to his objective, the pitch trajectory being online defined to achieve the tracking of elevation/travel desired trajectories. The controller scheme used in [11–13] has been modified in the current paper in order to prove the stability of the closed-loop system (which has not been formally established in the previous papers). The proposed controller is based on adaptive second-order sliding mode, which allows to obtain robust behavior with respect to modeling errors, uncertainties, and perturbations, while having reduced magnitude gain, which is dynamically adapted. It is well known that sliding mode control is robust with respect to perturbations and uncertainties and is simple to be tuned (high gain approach by considering the 'worst' case). Unfortunately, high frequency oscillations of the control input, the so-called chattering phenomenon, appear and can damage the actuators. In order to reduce this phenomenon, to improve the accuracy, and to ensure finite time convergence to the control objective, high-order sliding mode control appears at the beginning of 1990s [14], especially second-order sliding mode controllers as twisting and super-twisting (STW) algorithms. The advantage of the STW algorithm versus the twisting one is that no time derivative of the sliding variable is required, which reduces the noise in the control input. In the current paper, an adaptive version of the STW controller is used [15, 16]. This adaptive algorithm allows a robust control without overestimating the control gains for a large class of nonlinear systems of relative degree 1 with bounded additive and multiplicative uncertainties perturbations whose bounds are unknown. Note that this latter feature is interesting given that it allows to reduce the identification procedure.

The controller proposed in the sequel is, to authors' best knowledge, the first one using adaptive second-order sliding mode approach for the three Euler angles (elevation, travel, and pitch). Note that, in previous results [11, 12], first-order adaptive sliding mode controller or adaptive STW controllers for elevation and travel (the pitch angle being controlled by PD [11] or PID [12] controllers) have been experimentally evaluated. The controller proposed in the paper is increasing accuracy and robustness with respect to these latter given that the three angles are controlled by robust and adaptive controller. With respect to Plestan and Chriette [13], the current paper presents complete experimental results and a comparison with standard PID controllers; furthermore, as previously mentioned, a closed-loop system stability analysis is proposed (not made in [13]).

This paper is organized as follows. Section 2 describes the experimental set-up and its mathematical model. Section 3 displays the controller scheme, whereas Section 3.2 displays the adaptive sliding mode controller of attitude angles. Section 4 displays experimental results of the presented controller of the Quanser helicopter.

2. SYSTEM DESCRIPTION AND MODELS DESIGN OF THE EXPERIMENTAL SET-UP

The objective of this paper being to develop an attitude robust controller for a class of unmanned aerial vehicles, the experimental system described in the sequel is well adapted. In fact, this system is especially devoted to the control of the pitch, elevation, and travel angles.

2.1. Description of the system

The 3DOF helicopter studied in this work is shown in Figure 1 (parameters are given in Table I).

The system is composed of the helicopter body, which is a small arm with one propeller at each end, and the helicopter arm, which connects the body to a **fixed base**. Although the system cannot exhibit *translational motion*, as it is fixed in a support, it can *rotate freely about three axes*. The helicopter position is characterized by the pitch, travel, and elevation angles. The pitch movement corresponds to the rotation of the helicopter body about the helicopter arm; the travel movement corresponds to the rotation of the helicopter arm about the vertical axis, and the elevation movement corresponds to the rotation of the helicopter arm about the horizontal axis.

DOI: 10.1002/acs

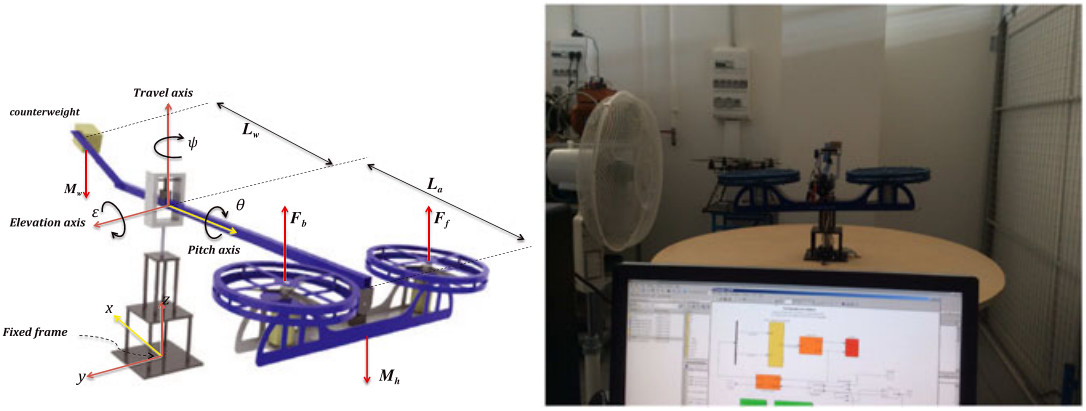

Figure 1. Left, schematic of Quanser 3DOF tandem helicopter. Right, experimental set-up (with the fan on the left-hand side, producing perturbations as wind gusts).

Table I. 3DOF helicopter system specifications [1].

Symbol	Description	Value	Unit
V_f and V_b	DC motor voltage of the front and back motors	$[-24\,;+24]$	V
K_F	Propeller force–thrust constant	0.1188	N/V
g	Gravity constant	9.81	$\mathrm{m\cdot s^2}$
M_h	Mass of the helicopter	1.426	kg
M_w	Mass of the counterweight	1.87	kg
L_a	Distance between travel axis to helicopter body	0.660	m
L_w	Distance between travel axis to the counterweight	0.470	m
L_h	Distance between pitch axis to each motor	0.178	m
J_ε	Moment of inertia about elevation	1.0348	$\mathrm{kg\cdot m^2}$
J_θ	Moment of inertia about pitch	0.0451	$\mathrm{kg\cdot m^2}$
J_ψ	Moment of inertia about travel	1.0348	$\mathrm{kg\cdot m^2}$

This platform has two DC motors, which are mounted at the two ends of a rectangular frame and drive two propellers. The helicopter attitude is controlled by means of the thrust forces F_b and F_f, which are generated by the two propellers.
Notice that this system is an underactuated system, that is, this system has two control forces, whereas there are three DOFs represented by the three attitude angles (the *travel* angle ψ, the *elevation* angle ϵ, and the *pitch* angle θ).

2.2. *Dynamics*

In this section, some assumptions are introduced, which take into account the main dynamics and nonlinearities of the helicopter, to obtain a simplified model that will be used to design a controller of attitude of the 3DOF helicopter.

Assumptions.

- **(A1)** The travel and elevation axes are perpendicular;
- **(A2)** All the axes intersect in the same point, which is considered as the origin of the global coordinate frame;
- **(A3)** The helicopter frame and counterweight mass centers are collinear with respect to the pitch axis;
- **(A4)** Joint friction, air resistance, and centrifugal forces are neglected;
- **(A5)** The thrust force is proportional to the motor voltage, and motors/propellers dynamics are neglected; and
- **(A6)** There are external perturbations acting on the helicopter (wind gust).

DOI: 10.1002/acs

Note that, in the experimental set-up, there is a deviation between pitch axis and the intersection of the travel/elevation axes. This geometric fact is not taken into account (Assumptions A1–A3) in the model in order to simplify this latter and to obtain a model usable for control design. Then, a robust control is required to overcome these constraints and uncertainties. Assumption A5 induces that the produced thrusts are proportional to the voltages applied to DC motors, that is,

$$\begin{bmatrix} F_f \\ F_b \end{bmatrix} = \begin{bmatrix} K_F V_f \\ K_F V_b \end{bmatrix} \tag{1}$$

with K_F as the propeller force–thrust constant. This assumption implies that the motors are exactly the same, which is not the case in the experimental set-up. Furthermore, there are also external perturbations (wind) acting on the system, which must be taken into account in the control design (Assumption A6).

Then, from the aforementioned assumptions, a simplified model of the 3DOF helicopter is given by [11]

$$J_\epsilon \ddot{\epsilon} = g(M_h L_a - M_w L_w)\cos\epsilon + L_a \cos\theta \; u_1 + F_\epsilon \tag{2}$$

$$J_\theta \ddot{\theta} = L_h \; u_2 + F_\theta \tag{3}$$

$$J_\psi \ddot{\psi} = L_a \cos\epsilon \sin\theta \; u_1 + F_\psi \tag{4}$$

where the new controls are expressed in terms of the control forces as

$$\begin{bmatrix} u_1 \\ u_2 \end{bmatrix} = \begin{bmatrix} F_f + F_b \\ F_f - F_b \end{bmatrix}. \tag{5}$$

The functions F_ϵ, F_θ, and F_ψ depend on all the uncertainties and perturbations terms that are assumed to be bounded. Note that Assumption A4 considers that there is no friction, air resistance, and so on. It can be considered that the effects of the forces concerned by Assumption A4 are taken into account in the uncertainties/perturbations terms F_ϵ, F_θ, and F_ψ.

The operating domain of the dynamical model of the 3DOF helicopter, which takes into account the mechanical constraints, is defined as follows:

- Pitch angle θ is defined on the interval $-45° \leqslant \theta \leqslant +45°$; and
- Elevation angle ϵ is defined on $-27.5° \leqslant \epsilon \leqslant +30°$.

From the angle ψ-dynamics, it is not possible to control travel angle when $\theta = 0$. Then, it is necessary to produce a pitch motion in order to change travel angle. It is a key point in the design of the attitude controller.

3. DESIGN OF ATTITUDE CONTROLLER

This section describes the scheme of the attitude controller knowing that, given the model (2),

- The elevation and travel dynamics directly depend on the pitch value and are actuated by the same control input u_1;
- The control input u_2 is acting on pitch dynamics; and
- The system is underactuated: three DOFs for only two control inputs.

3.1. Structure of the controller

All these previous items imply that it is necessary to design a control scheme in order to control the three DOFs with only two control inputs. A standard way consists, for the user, in defining first elevation and travel desired trajectories (which are the more natural trajectories to design *a priori*): then, based on an internal loop, a desired trajectory for the pitch is derived. Note that this pitch

DOI: 10.1002/acs

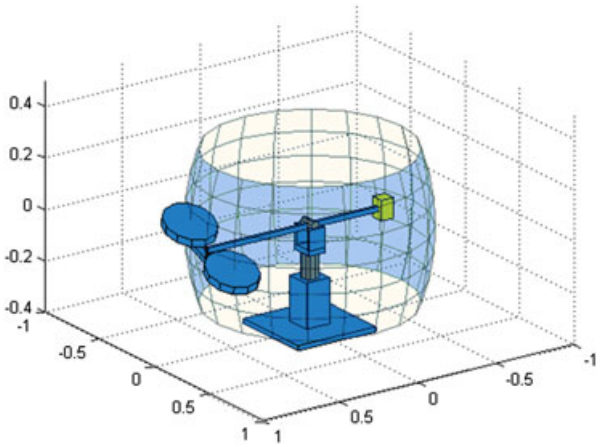

Figure 2. Helicopter 3D view with its workspace (light blue).

trajectory will have an impact not only on the travel dynamics but also on the elevation. The strategy for the design of the desired pitch trajectory has been initiated/used in [11, 13, 17], and an improved version is presented in the sequel of this section.

The system can be considered as a point mass mounted at the end of the arm, in the middle between two rotors axes. In such case, its position could be completely defined in a two-dimensional spherical workspace (Figure 2) by the travel and elevation angles. This simplified system has only two DOFs, and it can be controlled with two forces along the travel and elevation directions.

The main idea of the controller consists in defining 'virtual' control inputs allowing to linearize and decouple, by an input–output point of view, the system: by this way, the system will be viewed as three perturbed double integrators, each double integrator conceding an attitude angle. Then, a new control is proposed by defining the following 'virtual' control vector

$$\nu(u_1, \epsilon, \theta) = \begin{bmatrix} \nu_1 \\ \nu_2 \end{bmatrix}$$

such that

$$\begin{aligned} \nu_1 &= u_1 \cos\epsilon \sin\theta \\ \nu_2 &= u_1 \cos\theta. \end{aligned} \tag{6}$$

Given the working domain, it yields

$$\operatorname{sign}(u_1) = \operatorname{sign}(\nu_2).$$

From (2), it yields

$$\begin{aligned} J_\psi \ddot{\psi} &= L_a \nu_1 + F_\psi \\ J_\epsilon \ddot{\epsilon} &= G \cos\epsilon + L_a \nu_2 + F_\epsilon \\ J_\theta \ddot{\theta} &= L_h u_2 + F_\theta \end{aligned} \tag{7}$$

with $G = g(M_h L_a - M_w L_w)$. Then, by defining

$$\nu_1^* = \nu_1, \quad \nu_2^* = \frac{1}{L_a}\left[L_a \nu_2 + G\cos\epsilon\right], \tag{8}$$

one obtains

$$\begin{aligned} J_\psi \ddot{\psi} &= L_a \nu_1^* + F_\psi \\ J_\epsilon \ddot{\epsilon} &= L_a \nu_2^* + F_\epsilon \\ J_\theta \ddot{\theta} &= L_h u_2 + F_\theta. \end{aligned} \tag{9}$$

DOI: 10.1002/acs

To summarize, thanks to the previous control strategy, we have as follows:

- The nonlinear system (2) is transformed into the decoupled system (9), that is, ψ, ϵ, and θ are respectively independently controlled by ν_1^*, ν_2^*, and u_2. Note that the two equations of (6) are not independent but are linked through u_1;
- Dynamical equation of each angle is composed of a well-known term (named 'nominal') and an uncertain term; for example, for travel angle, one has

$$\ddot{\psi} = \underbrace{\frac{L_a}{J_\psi}\nu_1^*}_{\text{Nominal term}} + \underbrace{\frac{F_\psi}{J_\psi}}_{\text{Uncertain term}}$$

- The control inputs ν_1, ν_2 (and then ν_1^* and ν_2^*), and u_2 have to be chosen in order to stabilize the system (9) in spite of uncertainties and perturbations.

A key point is the computation of u_1 (which is the single function (with u_2) on which one can act) which allows that equation (6) are fulfilled. From (6), one acquires

$$u_1^2 \sin^2\theta = \frac{\nu_1^2}{\cos^2\epsilon} \quad \text{and} \quad u_1^2\cos^2\theta = \nu_2^2. \tag{10}$$

It yields

$$u_1^2 = \frac{\nu_1^2}{\cos^2\epsilon} + \nu_2^2 \tag{11}$$

Then, one has

$$u_1 = S\cdot\sqrt{\frac{\nu_1^2}{\cos^2\epsilon} + \nu_2^2} \tag{12}$$

with S defined as (this variable has been defined by a different manner than [11–13]; the new definition allows the proof of closed-loop system stability)

$$S = \begin{cases} \text{sign}(\nu_2) & \text{if } \nu_2 \neq 0 \\ 0 & \text{if } \nu_2 = 0. \end{cases} \tag{13}$$

Recall that, given the definition of ν_2 and the working domain, one has $\text{sign}(\nu_2) = \text{sign}(u_1)$. Furthermore, from (6), it is obvious that θ has to verify

$$\tan\theta = \frac{\nu_1}{\cos\epsilon\,\nu_2}. \tag{14}$$

Then, a way to decouple the system as (7) consists in forcing, thanks to the control input u_2, the angle θ to track the desired trajectory

$$\theta_d(t) = \tan^{-1}\left(\frac{\nu_1}{\cos\epsilon\,\nu_2}\right), \tag{15}$$

whereas the control input u_1 reads as (12). This control strategy allows to define the attitude controller scheme as follows (Figure 3):

- The first part of the controller allows to compute the control inputs ν_1 and ν_2 from the tracking errors between ψ and ϵ and their desired trajectories $\psi_d(t)$ and $\epsilon_d(t)$ (through ν_1^* and ν_2^*)

$$\nu_1 = \nu_1^*, \quad \nu_2 = \frac{1}{L_a}\left[L_a\nu_2^* - G\cos\epsilon\right]. \tag{16}$$

DOI: 10.1002/acs

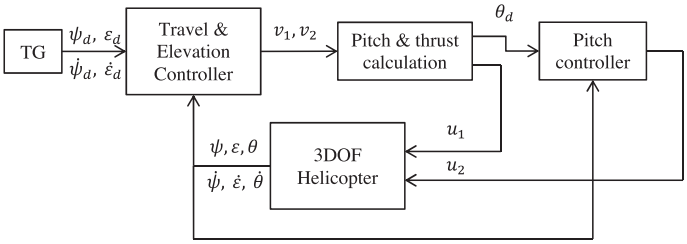

Figure 3. Attitude controller scheme.

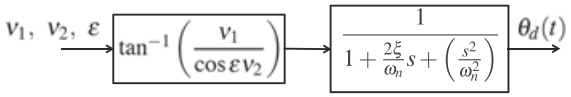

Figure 4. Computation scheme for pitch desired trajectory.

- From the previous stage, one firstly obtains the control input u_1 from (12). Secondly, this stage provides the pitch desired trajectory $\theta_d(t)$ from (15). From this latter desired trajectory, the pitch controller allows to provide u_2.

Desired trajectories features. The both desired trajectories for elevation and travel, respectively $\epsilon_d(t)$ and $\psi_d(t)$, are defined by the user: one supposes that they are defined sufficiently differentiable (at least twice). Given that the pitch desired trajectory is derived from (15), its smoothness has to be ensured. It has been made thanks to the addition of a second-order filter that gives the desired trajectory as shown by Figure 4. In conclusion, the desired trajectories $\theta_d(t)$, $\epsilon_d(t)$, and $\psi_d(t)$ are at least twice differentiable.

3.2. Design of the robust attitude controllers

In this section, control inputs v_1^*, v_2^*, and u_2 are designed in order to track respectively the desired trajectories $\psi_d(t)$, $\epsilon_d(t)$, and $\theta_d(t)$; u_1, v_1, and v_2 being derived from (12)–(16).
As shown in the following, the control inputs v_1^*, v_2^*, and u_2 are based on adaptive STW algorithm. The choice of such control strategies has been made in order to acquire a robust trajectory tracking for elevation, travel, and pitch. Furthermore, the adaptive feature allows to reduce the identification effort given that this strategy is applicable with a very reduced knowledge of perturbations and uncertainties.

Additionally, the control of pitch angle is quite sensitive and too much 'aggressive' control law could engender unstable behavior of the system. This fact can reduce the interest to use robust discontinuous control laws as first-order sliding mode order. A way to have a robust controller and also the robustness features of sliding mode is the use of second-order sliding mode controller. Additionally, the proposed controller is adaptive, which limits the magnitude of the control input (and then the chattering); the use of STW algorithm is also limiting the intrinsic discontinuous behavior of the control given that it does not use the time-derivative of the sliding variable as standard second-order sliding mode controllers.

3.2.1. Adaptive super-twisting algorithm [16]. Consider a single-input uncertain nonlinear system

$$\dot{x} = f(x) + h(x)u \tag{17}$$

with $x \in IR^n$ the state vector, $u \in IR$ the control input. Functions $f(x)$ and $h(x)$ are differentiable partially known vector-fields. Suppose that

(H1) The sliding variable $\sigma = \sigma(x,t) \in IR$ is designed so that the control objectives is fulfilled so if $\sigma = \sigma(x,t) = 0$;
(H2) The system (17) has a relative degree equal to one with respect to σ, and the internal dynamics are stable.

DOI: 10.1002/acs

Therefore, the sliding variable dynamics reads as

$$\dot{\sigma} = \underbrace{\frac{\partial \sigma}{\partial t} + \frac{\partial \sigma}{\partial x} f(x)}_{\varphi(x,t)} + \underbrace{\frac{\partial \sigma}{\partial x} h(x)}_{\gamma(x,t)} u = \varphi(x,t) + \gamma(x,t)u \tag{18}$$

(H3) The functions $\varphi(\cdot)$ and $\gamma(\cdot)$ are uncertain and bounded and read as

$$\varphi(\cdot) = \varphi_0(\cdot) + \Delta\varphi(\cdot), \quad \gamma(\cdot) = \gamma_0(\cdot) + \Delta\gamma(\cdot) \tag{19}$$

with φ_0, γ_0 the known nominal terms and $\Delta\varphi$, $\Delta\gamma$ the uncertain parts. The function $\gamma(\cdot)$ is such that

$$0 < \gamma_m < \gamma_0(\cdot) < \gamma_M < \infty, \quad |\Delta\gamma| < \gamma_0,$$

whereas the function φ fulfills $|\varphi_0| < \varphi_M$ and $|\Delta\varphi| < \Delta\varphi_M$ with φ_m, φ_M, φ_0, φ_M, $\Delta\varphi_M$ unknown real constants.

Given the choice of second-order sliding mode control strategy, the problem consists in driving the sliding variable σ and its derivative $\dot{\sigma}$ to zero in finite time in spite of the uncertainties/perturbations and their unknown boundaries described in (A3), by means of a continuous control.
The standard sliding mode and second-order sliding mode controllers, including the continuous STW algorithm, can robustly handle such problem if the boundaries of the perturbations are known. In this work, an adaptive-gain STW (ASTW) algorithm is developed: its gains are adapted to the unknown uncertainties/perturbations with the unknown boundaries and without control gain overestimation.

Definition 1
Consider the sliding variable σ and its dynamics (18). A real second-order sliding mode is established with respect to σ if there exists a finite time t_F such that, for $t \geqslant t_F$, one obtains $|\sigma| \leqslant \mu_1 T_e^2$ and $|\dot{\sigma}| \leqslant \mu_2 T_e$ with T_e the sampling period of the controller, μ_1, μ_2 positive constants. ■

The following STW control is considered [15, 16]:

$$u = -\alpha(t)|\sigma|^{1/2}\text{sign}(\sigma) + w, \quad \dot{w} = -\frac{\beta(t)}{2}\text{sign}(\sigma), \tag{20}$$

where the gains $\alpha(t)$ and $\beta(t)$ are online adjusted. The idea of designing ASTW is to dynamically increase the control gains $\alpha(t)$ and $\beta(t)$ until a second-order sliding mode with respect to σ is established. Then the gains shall start reducing. This gain reduction shall be reversed as soon as second-order sliding mode is lost (because of a too much small gain).

Sliding mode detector. A system named 'detector' is required to detect the occurrence of the sliding mode. A such system is constructed and incorporated in the ASTW control law that allows not overestimating the control gains $\alpha(t)$ and $\beta(t)$. This 'detector' is proposed through a domain $|\sigma| \leqslant \mu$ that is used as follows: as soon as this domain is reached, the gains $\alpha(t)$ and $\beta(t)$ start dynamically reducing until the system trajectories leave the domain. Then the gains start dynamically increasing in order to force the trajectories back to the domain in finite time. The main result is formulated in the following theorem.

Theorem 1 ([15, 16]*)*
Consider system (17) with the sliding variable $\sigma(x,t)$ and its associated dynamics (18). Suppose that Assumptions H1–H3 are fulfilled. Then, for any initial conditions $x(0), \sigma(0)$, there exists a positive constant μ such that a real second-order sliding mode with respect to $\sigma(x,t)$ is established $\forall t \geqslant t_F$ ($t_F < \infty$), thanks to the ASTW control (20) with the adaptive gains

$$\dot{\alpha} = \begin{cases} c_\alpha \text{sign}(|\sigma| - \mu), & \text{if } \alpha > \alpha_m \\ \alpha_m, & \text{if } \alpha \leqslant \alpha_m \end{cases}, \quad \beta = c_\beta \alpha, \tag{21}$$

where c_α and c_β are arbitrary positive constants.

DOI: 10.1002/acs

Remark 1
The second line of adaptation law (21) of α is used in order to ensure that the gains never become negative. Of course, it is interesting to tune α_m as small as possible, in order to be able to obtain small gains if necessary (when there are very reduced perturbations or uncertainties).

3.2.2. Control design and stability of the closed-loop system. The first step of the controller design consists in defining the sliding variables knowing that the relative degree of the system with respect to the sliding variable has to be equal to one. It yields

$$\begin{bmatrix} \sigma_\psi \\ \sigma_\epsilon \\ \sigma_\theta \end{bmatrix} = \begin{bmatrix} \left(\dot{\psi}(t) - \dot{\psi}_d(t)\right) + \lambda_\psi \left(\psi(t) - \psi_d(t)\right) \\ \left(\dot{\epsilon}(t) - \dot{\epsilon}_d(t)\right) + \lambda_\epsilon \left(\epsilon(t) - \epsilon_d(t)\right) \\ \left(\dot{\theta}(t) - \dot{\theta}_d(t)\right) + \lambda_\theta \left(\theta(t) - \theta_d(t)\right) \end{bmatrix}. \tag{22}$$

From (9), with $\sigma = [\sigma_\psi \ \sigma_\epsilon \ \sigma_\theta]^T$, one acquires the expression for $\dot{\sigma}$ as follows:

$$\dot{\sigma} = \begin{bmatrix} \frac{L_a}{J_\psi} v_1^* - \ddot{\psi}_d(t) + \lambda_\psi(\dot{\psi} - \dot{\psi}_d(t)) + \frac{F_\psi}{J_\psi} \\ \frac{L_a}{J_\epsilon} v_2^* - \ddot{\epsilon}_d(t) + \lambda_\epsilon(\dot{\epsilon} - \dot{\epsilon}_d(t)) + \frac{F_\epsilon}{J_\epsilon} \\ \frac{L_h}{J_\theta} u_2 - \ddot{\theta}_d(t) + \lambda_\theta(\dot{\theta} - \dot{\theta}_d(t)) + \frac{F_\theta}{J_\theta} \end{bmatrix}. \tag{23}$$

Assumptions H1–H2 are fulfilled. The control laws $[v_1^* \ v_2^* \ u_2]^T$ are inspired from (20)–(21) and are defined as

$$\begin{bmatrix} v_1^* \\ v_2^* \\ u_2 \end{bmatrix} = \begin{bmatrix} \frac{J_\psi}{L_a}\left(w_1^* - \lambda_\psi(\dot{\psi} - \dot{\psi}_d(t)) + \ddot{\psi}_d(t)\right) \\ \frac{J_\epsilon}{L_a}\left(w_2^* - \lambda_\epsilon(\dot{\epsilon} - \dot{\epsilon}_d(t)) + \ddot{\epsilon}_d(t)\right) \\ \frac{J_\theta}{L_h}\left(w_2 - \lambda_\theta(\dot{\theta} - \dot{\theta}_d(t)) + \ddot{\theta}_d(t)\right) \end{bmatrix} \tag{24}$$

with

$$\begin{aligned} w_1^* &= -\alpha_\psi(t)|\sigma_\psi|^{1/2}\text{sign}(\sigma_\psi) - \int_0^t \frac{\beta_\psi(\tau)}{2}\text{sign}(\sigma_\psi)\text{d}\tau \\ w_2^* &= -\alpha_\epsilon(t)|\sigma_\epsilon|^{1/2}\text{sign}(\sigma_\epsilon) - \int_0^t \frac{\beta_\epsilon(\tau)}{2}\text{sign}(\sigma_\epsilon)\text{d}\tau \\ w_2 &= -\alpha_\theta(t)|\sigma_\theta|^{1/2}\text{sign}(\sigma_\theta) - \int_0^t \frac{\beta_\theta(\tau)}{2}\text{sign}(\sigma_\theta)\text{d}\tau \end{aligned} \tag{25}$$

Stability analysis. The stability of the closed-loop system can be proved on two steps: first of all, the desired trajectories have to be smooth and, at least, twice differentiable; then, once the control input u_2, which is devoted to this single task, has made θ tracking $\theta_d(t)$ (or has forced θ reaching a vicinity of $\theta_d(t)$), it is necessary to be sure that the control input u_1, via v_1, v_2, v_1^*, v_2^*, makes ψ and ϵ tracking $\psi_d(t)$ and $\epsilon_d(t)$.

First step – smoothness of the desired trajectories. As written previously, desired trajectories $\psi_d(t)$ and $\epsilon_d(t)$ are defined by the user and supposed to be defined bounded and smooth. Furthermore, the desired trajectory $\theta_d(t)$ is also twice differentiable given its design (Figure 4). Assumption A3 is fulfilled in the working domain.

DOI: 10.1002/acs

Second step – control features. From (2)–(9), it is clear that the control input u_2 is acting, by an independent way, to θ-dynamics. Given the intrinsic nature of the ASTW algorithm, there exists a finite time such that θ is reaching $\theta_d(t)$ (or its vicinity).
Firstly, given that there exists a finite time such that $\theta(t) = \theta_d(t)$, it will be proved in the sequel that u_1 defined in (12) drives $\psi(t)$ and $\epsilon(t)$ to their desired trajectories $\psi_d(t)$ and $\epsilon_d(t)$ independently. Secondly, it will be proved that, early from θ is evolving in a vicinity of $\theta_d(t)$, then the system is sufficiently decoupled such that ν_1 and ν_2 force $\psi(t)$ and $\epsilon(t)$ to reach $\psi_d(t)$ and $\epsilon_d(t)$.
Suppose that $\theta(t) = \theta_d(t)$. Putting (15) into the last equation in (2), one acquires

$$\begin{aligned} J_\psi \ddot{\psi} &= L_a \cos\epsilon \frac{\frac{\nu_1}{\nu_2 \cos\epsilon}}{\sqrt{1+\frac{\nu_1^2}{\nu_2^2\cos^2\epsilon}}} u_1 + F_\psi \\ &= L_a \cos\epsilon \frac{\frac{\nu_1}{\nu_2 \cos\epsilon}}{\sqrt{1+\frac{\nu_1^2}{\nu_2^2\cos^2\epsilon}}} \sqrt{\frac{\nu_1^2}{\cos^2\epsilon}+\nu_2^2}\cdot \operatorname{sign}(\nu_2) + F_\psi \\ &= L_a \cdot \cos\epsilon \cdot \frac{\nu_1}{\nu_2\cos\epsilon} \cdot \frac{1}{\sqrt{1+\frac{\nu_1^2}{\nu_2^2\cos^2\epsilon}}} \cdot \sqrt{1+\frac{\nu_1^2}{\nu_2^2\cos^2\epsilon}} \cdot |\nu_2| \operatorname{sign}(\nu_2) + F_\psi \\ &= L_a \nu_1 + F_\psi. \end{aligned} \tag{26}$$

In this case, the control input ν_1, which is based on ASTW control ($\nu_1 = \nu_1^*$), ensures that, in a finite time, ψ reaches $\psi_d(t)$; furthermore, a real second-order sliding mode with respect to σ_ψ is established in a finite time.
By a similar way, putting (15) into the first equation in (2) and with $G = g(M_h L_a - M_w L_w)$, one acquires

$$\begin{aligned} J_\epsilon \ddot{\epsilon} &= G\cos\epsilon + L_a \cos\left[\tan^{-1}\left(\frac{\nu_1}{\nu_2\cos\psi}\right)\right]\cdot u_1 + F_\epsilon \\ &= G\cos\epsilon + L_a \cdot \frac{1}{\sqrt{1+\frac{\nu_1^2}{\nu_2^2\cos^2\epsilon}}} \cdot \sqrt{\frac{\nu_1^2}{\cos^2\epsilon}+\nu_2^2}\cdot \operatorname{sign}(\nu_2) + F_\psi \\ &= G\cos\epsilon + L_a \cdot \frac{1}{\sqrt{1+\frac{\nu_1^2}{\nu_2^2\cos^2\epsilon}}} \cdot \sqrt{1+\frac{\nu_1^2}{\nu_2^2\cos^2\epsilon}} \cdot |\nu_2| \cdot \operatorname{sign}(\nu_2) + F_\psi \\ &= G\cos\epsilon + L_a \cdot \nu_2 + F_\psi. \end{aligned} \tag{27}$$

From (8), given that the control input ν_2 reads as

$$\nu_2 = \frac{1}{L_a}\left[L_a \nu_2^* - G\cos\epsilon\right]$$

and is based on ASTW control (25), it is clear that there exists a finite time such that a real second-order sliding mode with respect to σ_ϵ is established.

Suppose now that θ is evolving in a vicinity of $\theta_d(t)$. In fact, thanks to u_2, a real second-order sliding mode with respect to σ_θ is established. It means that the pitch angle θ can be considered as

$$\theta = \theta_d(t) + \delta\theta$$

with $\delta\theta$ representing the tracking 'error'. Given the robustness and the accuracy feature of the control, and given the working domain, it is reasonable to consider that $\delta\theta$ is small. By making similar

DOI: 10.1002/acs

computations as previously, by considering $\theta = \theta_d(t) + \delta\theta$, one has

$$\begin{aligned} \ddot{\psi} &= \frac{1}{J_\psi}\left[L_a \nu_1 \cos(\delta\theta) + L_a \cos(\epsilon)\sin(\delta\theta)\nu_2 + F_\psi\right] \\ \ddot{\epsilon} &= \frac{1}{J_\epsilon}\left[G\cos(\epsilon) + L_a\cos(\delta\theta)\nu_2 + \frac{L_a \sin(\delta\theta)}{\cos(\epsilon)}\nu_1 + F_\epsilon\right], \end{aligned} \tag{28}$$

which gives

$$\begin{bmatrix} \ddot{\psi} \\ \ddot{\epsilon} \end{bmatrix} = \underbrace{\begin{bmatrix} L_a\cos(\delta\theta) & L_a\cos(\epsilon)\sin(\delta\theta) \\ \dfrac{L_a\sin(\delta\theta)}{\cos\epsilon} & L_a\cos(\delta\theta) \end{bmatrix}}_{A} \cdot \begin{bmatrix} \nu_1 \\ \nu_2 \end{bmatrix} + \begin{bmatrix} 0 \\ G\cos(\epsilon) \end{bmatrix} + \begin{bmatrix} F_\psi \\ F_\epsilon \end{bmatrix}. \tag{29}$$

It is clear that we have as follows:

- If $\delta\theta = 0$ (i.e., θ is exactly tracking the desired trajectory θ_d), then the system is fully decoupled. It is the previous case; and
- If $\delta\theta \neq 0$, the matrix A is a diagonal-dominant one which allows to 'sufficiently' decoupled the dynamics of ϵ and ψ. In fact, given the working domain, one has $0.88 < \cos(\epsilon) < 1$; furthermore, it is reasonable to consider $|\delta\theta|$ reduced, which gives $\cos(\delta\theta) >> \sin(\delta\theta)$. Then, it yields

$$\begin{aligned} L_a\cos(\delta\theta) &> L_a\cos(\epsilon)\sin(\delta\theta) \\ L_a\cos(\delta\theta) &> L_a\sin(\delta\theta)/\cos(\epsilon). \end{aligned} \tag{30}$$

4. EXPERIMENTAL RESULTS

4.1. Experimental process description and controller parameters tuning

The experimental set-up (mechanical parameters, inputs features) has been described in Section 2.1. By a technological point of view, the equipment is the following: PC Dell mod. Precision 390 (Intel Core 2 DUO, 1.60 GHz, 2 Go RAM), Matlab 2009*a*, Matlab Simulink, and sampling time $T_e = 0.01$ s. An external perturbation is applied to the helicopter thanks to a fan (Figure 1, right-hand side); this fan being located in order to provide wind in side direction, that is, it is mainly acting on the travel and pitch angles. For the validation of the designed controllers, stabilization and trajectories tracking are considered. For the trajectories tracking, desired trajectories for elevation and travel, respectively $\epsilon_d(t)$ and $\psi_d(t)$, are used, the desired trajectory $\theta_d(t)$ of the pitch angle being computed online by an inner loop. The trajectories used in the sequel are time-varying desired angles defined by two sinus waves (Figure 5). The elevation wave period is two times greater than the travel wave period; by this way, the desired trajectory in the (ψ, ϵ)-workspace is cyclic and form a turned 8-like pattern. Note that these trajectories are designed by taking into account constraints on maximal values of velocity, acceleration, and control inputs. Front and back control motor voltages are derived from (1) and (5)

$$V_f = \frac{1}{2K_F}(u_1 + u_2), \quad V_b = \frac{1}{2K_F}(u_1 - u_2). \tag{31}$$

The sliding variables (22) parameters have been tuned as $\lambda_\psi = 2$, $\lambda_\epsilon = 3$ and $\lambda_\theta = 1$. The adaptive STW controllers' parameters for attitude controllers (20)–(21) are respectively defined as described in Table II. The choice of these parameters has been made in order to obtain accurate and robust results. Note that the parameter, which has to be tuned by a very careful manner, is μ. In fact, the sliding mode detection has been chosen not too large because it could induce an inaccurate result, and not too small because it could induce very large increase of the gains $\alpha(t)$ and $\beta(t)$ (and possibly

DOI: 10.1002/acs

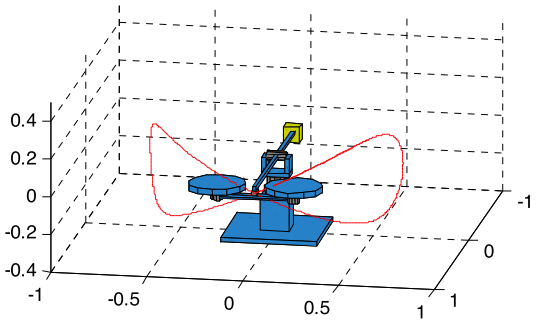

Figure 5. 3D desired trajectory. Sinusoidal trajectories.

Table II. Parameters of the attitude controller based on adaptive super-twisting algorithm.

Parameters	c_α	c_β	μ	α_m
Travel ψ	0.1	0.2	0.1	0.2
Elevation ϵ	1	0.2	0.1	0.2
Pitch θ	0.1	0.2	0.1	0.2

an instability). The tuning of μ particularly depends on the sampling time T_e (in the case of first-order sliding mode control, this point has been detailed in [18]). The parameter α_m is used only to ensure a minimal value of the gain, whereas parameters c_α and c_β are acting on the dynamics of the gains. In future works, methodologies for the tuning of all the parameters will be studied.

4.2. *Experimental validation*

In order to show the efficiency and the robustness of the proposed control solution, a comparison between the ASTW controller and a PID one is presented in the sequel. For the PID controllers, the control inputs v_1^*, v_2^*, and u_2 read as (24) with

$$\begin{aligned} w_1^* &= K_{p_\psi} e_\psi + K_{i_\psi} \int_{t_0}^{t} e_\psi \mathrm{d}\tau + K_{d_\psi} \frac{\mathrm{d}e_\psi}{\mathrm{d}t} \\ w_2^* &= K_{p_\epsilon} e_\epsilon + K_{i_\epsilon} \int_{t_0}^{t} e_\epsilon \mathrm{d}\tau + K_{d_\epsilon} \frac{\mathrm{d}e_\epsilon}{\mathrm{d}t} \\ w_2 &= K_{p_\theta} e_\theta + K_{i_\theta} \int_{t_0}^{t} e_\theta \mathrm{d}\tau + K_{d_\theta} \frac{\mathrm{d}e_\theta}{\mathrm{d}t} \end{aligned} \tag{32}$$

with

- e_ψ, e_ϵ, and e_θ the tracking errors of travel, elevation, and pitch angles, respectively;
- K_{p_ψ}, K_{p_ϵ}, and K_{p_θ} the proportional gains of travel, elevation, and pitch angles, respectively;
- K_{i_ψ}, K_{i_ϵ}, and K_{i_θ} the integral gains of travel, elevation and pitch angles, respectively; and
- K_{d_ψ}, K_{d_ϵ}, and K_{d_θ} the derivative gains of travel, elevation, and pitch angles, respectively.

The gains of PID controllers have been tuned by taking into account pole placement rules. The PID controller gains are defined from ($*$ being ψ, ϵ, and θ)

$$K_{p_*} = 3a_*\omega_*^2, \qquad K_{d_*} = 3a_*\omega_*, \qquad K_{i_*} = \zeta_* a_* \omega_*^3$$

with tuned parameters detailed in Table III.

The experimental tests have been made with perturbation produced by the fan at around $t = 100$ s. Figures 6 and 7 display the trajectories of attitudes angles and the control inputs. Figure 8 displays the evolution of the ASTW controller gains: it can be viewed that the gains are evolving versus

DOI: 10.1002/acs

Table III. Parameters of the attitude PID controllers.

Parameter	a_*	ω_*	ζ_*
Travel ψ	J_ψ / L_a	0.6	0.25
Elevation ϵ	J_ϵ / L_a	1.6	0.15
Pitch θ	J_θ / L_h	6	0.1

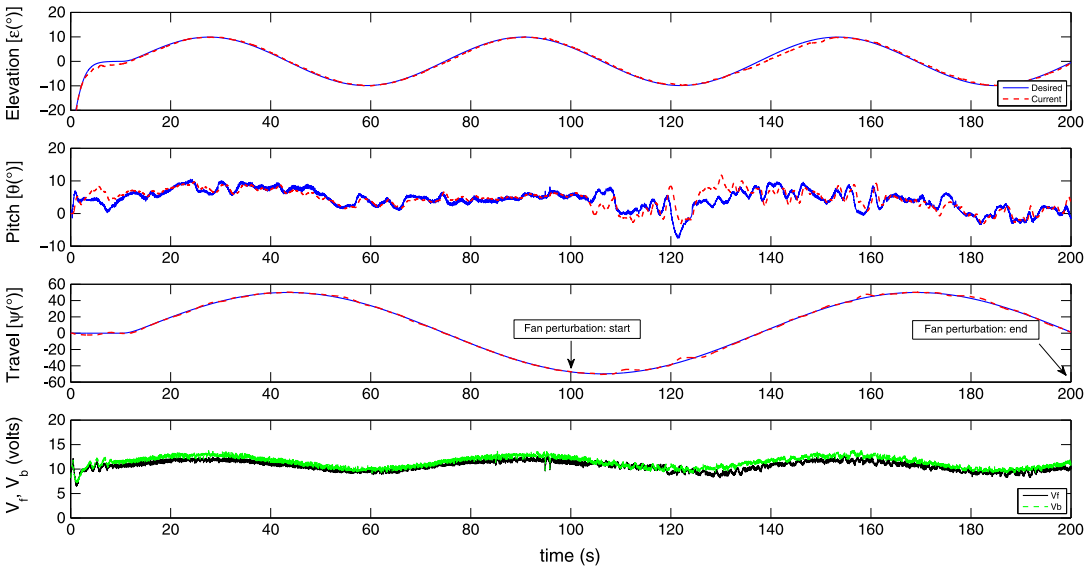

Figure 6. Adaptive super-twisting control – experimental results for trajectory tracking.

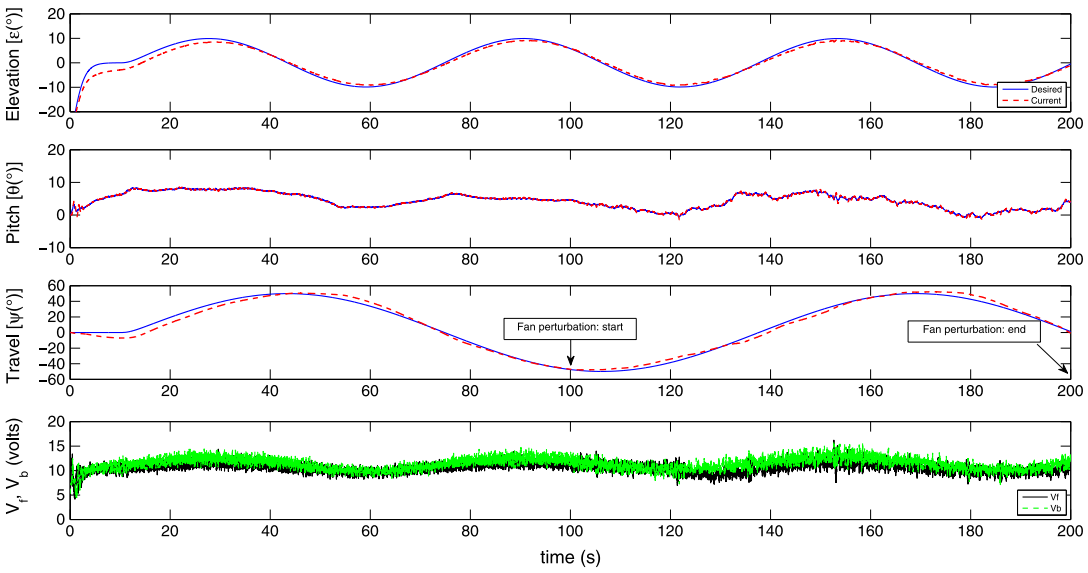

Figure 7. PID control – experimental results for trajectory tracking.

perturbation. Figures 9 and 10 display results obtained for the stabilization. All the results show the efficiency of the both controllers in spite of the perturbations. The pitch angle dynamics appears to be higher with the ASTW controller, but remains in reasonable domain ($\pm$ 10°). However, the attention has to be focused on the travel/elevation tracking given that they are the key variables to be controlled. In order to precisely analyze the performances, several information have been computed for both controllers, for $t \in [80\,\text{s}, 200\,\text{s}]$

DOI: 10.1002/acs

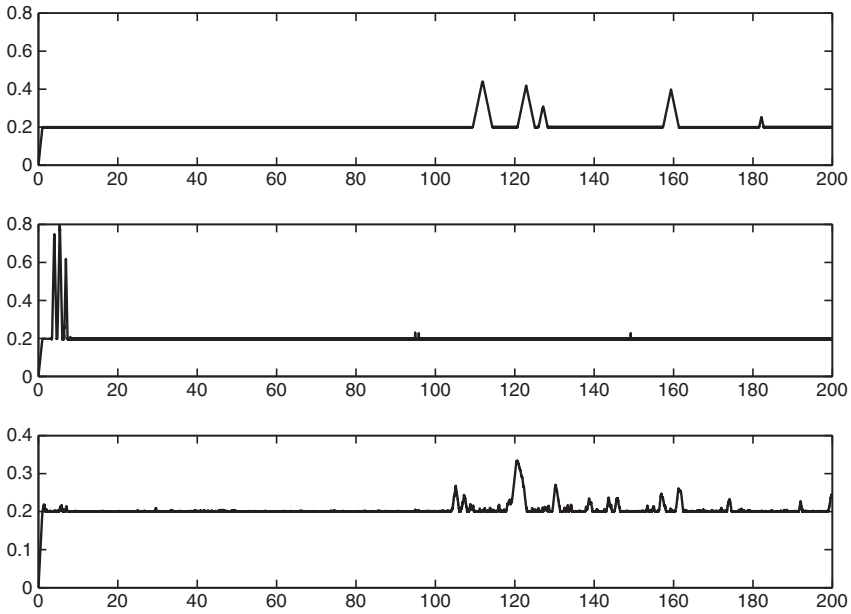

Figure 8. Adaptive super-twisting control. Top, gain α_ψ versus time (s). Middle, gain α_ϵ versus time (s). Bottom, gains α_θ versus time (s).

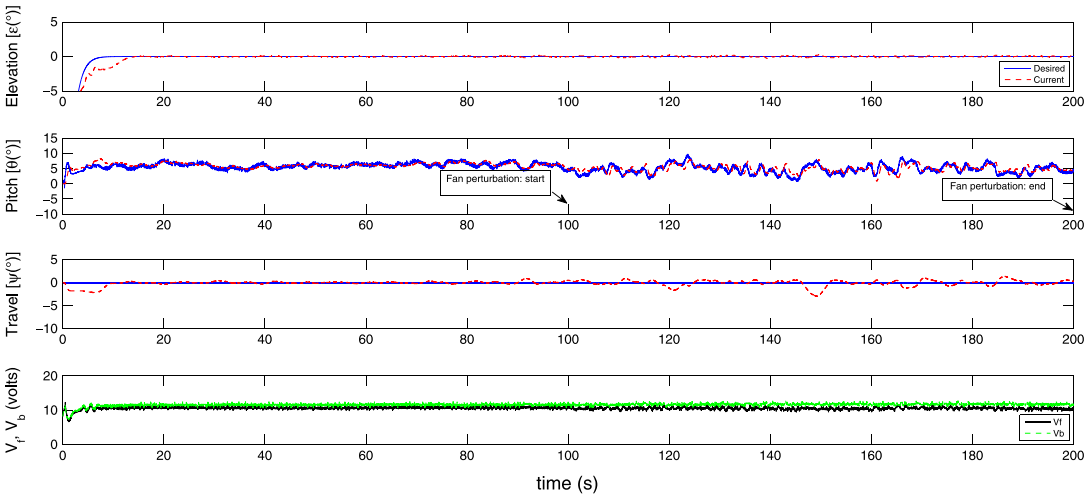

Figure 9. Adaptive-gain super-twisting control – experimental results for stabilization.

- Mean and standard variation of the absolute value of tracking errors, for the three angles (Tables IV and V) – it allows to quantify the quality of the tracking; and
- Mean and standard variation of the voltage control inputs V_f and V_b (Table VI) – it allows to quantify the amount of used energy. This information is interesting in case of autonomous flight.

Analysis of all these results yields the following comments:

- The performances of the ASTW controller are better, in terms of accuracy, for elevation and travel angles, which are the outputs on which the user has focused his interest (definition of the desired trajectories). With ASTW controller, the mean and the standard deviation of the errors for these both angles are smaller. Concerning the pitch angle, which is a secondary hidden output for the user, PID controller appears to give better results.

DOI: 10.1002/acs

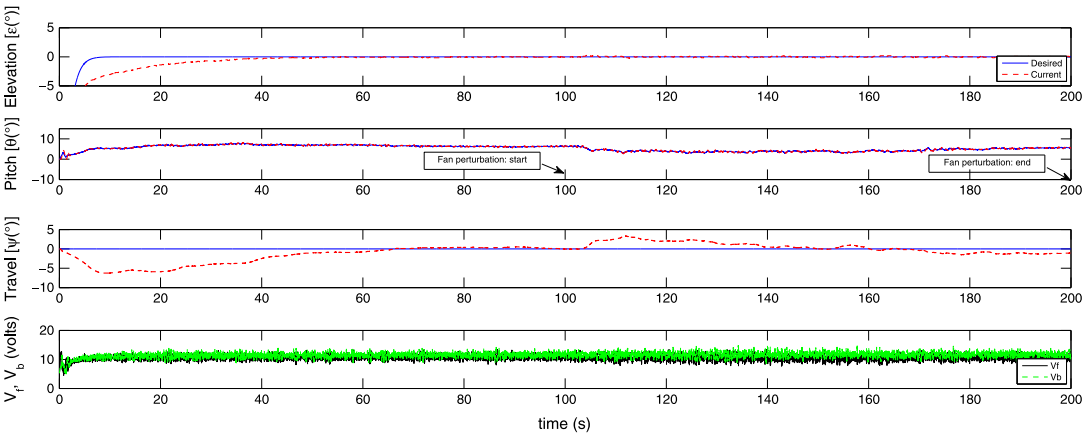

Figure 10. PID control – experimental results for stabilization.

Table IV. Evaluation of the performances of ASTW/PID controllers – mean of stabilization/tracking error absolute values of elevation, pitch, and travel angles for $t \in [80\,\text{s}; 200\,\text{s}]$.

Evaluation criteria	Mean ($\lvert e_\epsilon \rvert$) (°)	Mean ($\lvert e_\theta \rvert$) (°)	Mean ($\lvert e_\psi \rvert$) (°)
PID controller + stabilization	0.0654	4.6596	0.9959
ASTW controller + stabilization	0.0670	4.9736	0.4372
PID controller + traj. tracking	0.6693	5.1469	2.5658
ASTW controller + traj. tracking	0.3943	5.8239	0.8233

Table V. Evaluation of the performances of ASTW/PID controllers – standard deviation of stabilization/tracking error of elevation, pitch and travel angles for $t \in [80\,\text{s}; 200\,\text{s}]$.

Evaluation criteria	Std (e_ϵ) (°)	Std (e_θ) (°)	Std (e_ψ) (°)
PID controller + stabilization	0.0848	1.0353	1.2099
ASTW controller + stabilization	0.0874	1.5157	0.6357
PID controller + traj. tracking	0.7438	4.9558	3.0333
ASTW controller + traj. tracking	0.5442	5.7468	1.2599

Table VI. Evaluation of the performances of ASTW/PID controllers – average and standard deviation of control inputs (V) for $t \in [80\,\text{s}; 200\,\text{s}]$.

Evaluation criteria	Mean (V_f) (V)	Std (V_f) (V)	Mean (V_b) (V)	Std (V_b) (V)
PID controller + stabilization	10.61	0.85	11.48	0.96
ASTW controller + stabilization	10.58	0.40	11.59	0.45
PID controller + traj. tracking	10.67	1.08	11.35	1.24
ASTW controller + traj. tracking	10.65	0.96	11.37	1.11

ASTW, adaptive-gain super-twisting.

- Both controllers require similar means for V_f and V_b, whereas the standard deviation is lower for ASTW. It means that the voltage input has a lower level of oscillation, which is a positive feature for the actuator, its dynamics, and for the consumed energy.

DOI: 10.1002/acs

To summarize, on the proposed benchmark (trajectory tracking and stabilization), ASTW controller appears to provide better results in term of accuracy for elevation and travel angles without any knowledge of the uncertainties/perturbations and for quality of the control inputs. PID controller induces lower pitch angle.

5. CONCLUSION

This paper presents a robust controller for a 3DOF helicopter; the controller is based on a scheme of autopilot and is using adaptive second-order sliding mode controller for each attitude angle. The adaptive version of STW control does not require knowledge of uncertainties/perturbations. Experimental results show the efficiency of the control. In future works, adaptive high-order (at least third) sliding mode controller will be developed in order to improve the accuracy and the robustness of the closed-loop system. Methodologies for parameters' tuning will be also studied in order to simplify the controller design.

ACKNOWLEDGEMENTS

The authors acknowledge the support of the ANR grant CHASLIM (ANR-11-BS03-0007). The paper is also a part of a Postgraduate Cooperation Program (PCP) between Ecole Centrale de Nantes, the Autonomous University of Nuevo Leon (UANL), and Ripple Motion company. Madhumita Pal is financially supported by EU HERITAGE program.

REFERENCES

1. Quanser. 3-DOF helicopter reference manual. *Technical Report ,* Quanser Consulting Inc.: Markham, 2006.
2. Ishitobi M, Nishi M, Nakasaki K. Nonlinear adaptive model following control for a 3-DOF tandem-rotor model helicopter. *Control Engineering Practice* 2010; **18**(8):936–943.
3. Meza-Sánchez IM, Aguilar LT, Shiriaev A, Freidovich L, Orlov Y. Nonlinear output feedback h_∞-tracking control of a 3-DOF underactuated helicopter. In *IFAC World Congress*, Milano, Italy, 2011.
4. Andrievsky B, Peaucelle D, Fradkov AL. Adaptive control of 3DOF motion for LAAS helicopter benchmark: design and experiments. *American Control Conference (ACC' 07)*, New York, USA, 2007.
5. Lopez R, Galvao R, Milhan A, Becerra V, Yoneyama T. Modelling and constrained predictive control of a 3DOF helicopter. *Congreso Brasileiro de Automatica*, Salvador-Bahia, Brazil, 2006.
6. Kutay AT, Calise AJ, Idan M, Hovakimyan N. Experimental results on adaptive output feedback control using a laboratory model helicopter. *IEEE Transactions on Control Systems Technology* 2005; **13**(2):196–202.
7. Avila-Vilchis J, Brogliato B, Dzul A, Lozano R. Nonlinear modeling and control of helicopters. *Automatica* 2003; **39**(9):1526–1530.
8. Heiges MW, Menon PKA, Schrage DP. Synthesis of a helicopter full-authority controller. *Journal of Guidance, Control, and Dynamics* 1992; **15**(1):222–227.
9. Snell SA, Enns DF, Garrard Jr WL. Nonlinear inversion flight control for a supermaneuvrable aircraft. *Journal of Guidance, Control, and Dynamics* 1992; **15**(4):976–984.
10. Bertrand S, Hamel T, Piet-Lahanier H. Stability analysis of an UAV controller using singular perturbation theory. In *IFAC World Congress*, Seoul, Korea, 2008.
11. Odelga M, Plestan F, Chriette A. Control of 3 DOF helicopter: a novel autopilot scheme based on adaptive sliding mode control. *American Control Conference*, Montreal, Canada, 2012.
12. Chriette A, Plestan F. Nonlinear modeling and control of a 3DOF helicopter. *Asme Biennal Conference on Engineering Systems Design and Analysis (ESDA)*, Nantes, France, 2012.
13. Plestan F, Chriette A. A robust autopilot based on adaptive super-twisting algorithm for a 3DOF helicopter. In *IEEE Conference on Decision and Control*, Maui, USA, 2012.
14. Levant A. Sliding order and sliding accuracy in sliding mode control. *International Journal of Control* 1993; **58**(6):1247–1263.
15. Shtessel Y, Plestan F, Taleb M. Super-twisting adaptive sliding mode control with not-overestimated gains : application to an electropneumatic actuator. In *IFAC World Congress*, Milano, Italy, 2011.
16. Shtessel Y, Taleb M, Plestan F. A novel adaptive-gain supertwisting sliding mode controller: methodology and application. *Automatica* 2012; **48**(5):759–769.
17. Guillo M. *mise en place d'une plateforme d'hélicoptère - modélisation, simulation et implantation de lois de commande. master th.no.2010-19 [in french]*. INSA Rennes: France, 2010.
18. Plestan F, Shtessel Y, Brégeault V, Poznyak A. New methodologies for adaptive sliding mode control. *International Journal of Control* 2010; **83**(9):1907–1919.

DOI: 10.1002/acs